Marine Micropaleontology 96–97 (2012) 48–62

Contents lists available at SciVerse ScienceDirect

Marine Micropaleontology

journal homepage: www.elsevier.com/locate/marmicro

Archaeperidinium saanichi sp. nov.: A new species based on morphological variation of cyst and theca within the *Archaeperidinium minutum* Jörgensen 1912 species complex

Kenneth Neil Mertens [a,*,1], Aika Yamaguchi [b,c,1], Hisae Kawami [d], Sofia Ribeiro [e], Brian S. Leander [b,c], Andrea Michelle Price [f], Vera Pospelova [f], Marianne Ellegaard [e], Kazumi Matsuoka [d]

[a] *Research Unit Palaeontology, Ghent University, Krijgslaan 281 s8, 9000 Gent, Belgium*
[b] *Department of Botany, University of British Columbia, #3529-6270 University Boulevard, Vancouver, BC, Canada V6T 1Z4*
[c] *Department of Zoology, University of British Columbia, #3529-6270 University Boulevard, Vancouver, BC, Canada V6T 1Z4*
[d] *Institute for East China Sea Research (ECSER), Nagasaki University, 1–14, Bunkyo-machi, Nagasaki, 852-8521, Japan*
[e] *Department of Biology, Faculty of Science, University of Copenhagen, Øster Farimagsgade 2D DK-1353 Copenhagen K, Denmark*
[f] *School of Earth and Ocean Sciences, University of Victoria, OEASB A405, P.O. Box 3065 STN CSC, Victoria, BC, Canada V8W 3V6*

ARTICLE INFO

Article history:
Received 11 April 2012
Received in revised form 14 August 2012
Accepted 16 August 2012

Keywords:
Dinoflagellate
Saanich Inlet
LSU rDNA
Single-cell PCR
Spiny brown cyst
SSU rDNA

ABSTRACT

In this paper we describe a new species, *Archaeperidinium saanichi* sp. nov. within the *Archaeperidinium minutum* Jörgensen 1912 species complex. We examined the morphological variation of the cyst and motile stage by incubation experiments from sediment samples collected in coastal British Columbia (Canada), and compared it to closely related species. The theca of *A. saanichi* is differentiated from related species by overall size, the asymmetry of the intercalary plates and the right-sulcal plate (S.d.) not touching the cingulum. We provide a key to differentiate all closely related species. *A. saanichi* can be readily distinguished from *A. minutum* by a distinctively large cyst with a broad 2a type archeopyle and regularly spaced processes with relatively broad bases and aculeate process tips. Molecular phylogenetic analyses of large and small subunit (LSU and SSU) rDNA sequences demonstrated a close affinity of this species to *A. minutum*; however, the relatively high level of sequence conservation in dinoflagellate rDNA sequences made these particular markers inadequate for distinguishing one species from the other. Sediment-trap data suggest that *A. saanichi* has a preference for cooler temperatures and lowered salinities.

1. Introduction

Free-living marine dinoflagellates form a large group of eukaryotes, currently encompassing approximately 1555 species (Gómez, 2005). Some dinoflagellates form resting cysts as part of their sexual cycle, often to overcome unfavorable conditions (e.g. von Stosch, 1973). Linking these cysts to their respective motile stage is important for both biological and geological studies. This was traditionally established by incubation of living cysts and identifying the emergent motile stage (Wall and Dale, 1968). The advent of molecular techniques has provided an important accessory tool by single-cell PCR or single-cyst PCR (Bolch, 2001; Matsuoka et al., 2006a; Takano and Horiguchi 2006).

For the thecate heterotrophic genus *Protoperidinium*, which comprises 264 species (Gómez, 2005), only a few cyst-theca relationships have been established (e.g. Head, 1996). In recent years, further incubation studies have demonstrated more of these relationships for the genus *Protoperidinium* (e.g. Matsuoka et al., 2006b; Kawami and Matsuoka, 2009). Some of these cysts are distinctly round in shape, spine bearing, and brown in color; they are therefore called "spiny round brown cysts". Two cyst-based genera have been erected to classify these species. The first, *Echinidinium*, was erected by Zonneveld (1997). These cysts open with a theropylic archeopyle (i.e., an angular slit that follows paraplate boundaries but without complete release of plates) (Matsuoka, 1988; Head et al., 2001). The second, *Islandinium*, was erected by Head et al. (2001) and opens with a saphopylic archeopyle (i.e., having a free operculum) (Matsuoka, 1988).

For the "spiny round brown cysts" with theropylic archeopyles, cyst-motile relationships have been established for only very few species: *Protoperidinium monospinum* (Zonneveld and Dale, 1994), *Archaeperidinium minutum* Jörgensen, 1912 (Wall and Dale, 1968; Fukuyo et al., 1977; Ribeiro et al., 2010), and *Protoperidinium tricingulatum* (Kawami et al., 2009). However, species assigned to other genera have also been shown to form "spiny round brown cysts": *Pheopolykrikos hartmannii* (Matsuoka and Fukuyo, 1986,

* Corresponding author. Tel.: +32 92644613; fax: +32 92644608.
E-mail address: kenneth.mertens@ugent.be (K.N. Mertens).
[1] both authors have equal contributions to this paper.

0377-8398/$ – see front matter © 2012 Elsevier B.V. All rights reserved.
http://dx.doi.org/10.1016/j.marmicro.2012.08.002

retransferred to the genus *Polykrikos* by Hoppenrath et al., 2010) and *Oblea acanthocysta* (Kawami et al., 2006).

Archaeperidinium minutum Jörgensen, 1912 was first described by Kofoid (1907) from San Pedro Harbor, California, as *Peridinium minutum* Kofoid, 1907. Jörgensen (1912, p. 6) proposed the name *Archaeperidinium minutum* for this species, because he wanted to classify species based on the number of intercalary plates, which would place species of the then used name *Peridinium* with two intercalary plates within the genus *Archaeperidinium*; *Peridinium* was retained for species with three anterior intercalary plates. Abé, on the other hand, put more emphasis on the number and shape of the sulcal plates and proposed to classify *Peridinium minutum* within the *Monovela* group (Abé, 1936, p. 669–670; 1981, p. 304–307). After the reinstatement of the name *Protoperidinium*, the species was transferred to *Protoperidinium minutum* by Loeblich (1970, p. 905). Taylor (1976, p. 136–138) tried to compromise Jörgensen's and Abé's schemes by proposing three sections within the subgenus *Archaeperidinium*, one in which the girdle has no displacement, which he considered to correspond with the *Monovela* group of Abé. However, this is incorrect because Abé (1981, p. 305) considered the number of intercalary plates in the *Monovela* group to be either two or three. Recently, Yamaguchi et al. (2011) moved *Protoperidinium minutum* out of the genus *Protoperidinium* because of its separation from the remaining *Protoperidininum* species in phyologenies based on small subunit and large subunit (SSU and LSU) ribosomal DNA (rDNA) sequences and reinstated the name *Archaeperidinium minutum* Jörgensen, 1912. *Archaeperidinium minutum* is considered widespread, found in tropical to boreal areas (Okolodkov, 2005), which suggests the possible presence of multiple species within this species complex.

In this paper, we describe the theca and cyst of a new species, *Archaeperidinium saanichi*, through germinating spiny brown cysts from surface sediments from coastal British Columbia, obtaining LSU and SSU rDNA sequences, and studying sediment trap samples from Saanich Inlet and Effingham Inlet.

2. Materials and methods

2.1. Germination experiment

For incubation experiments, sediment samples containing spiny brown cysts were collected at three locations around southern Vancouver Island: (1) Camera Station near the VENUS (Victoria Experimental Network Under the Sea) sediment trap in Patricia Bay (Site A), (2) Oak Bay (Site B) and (3) Patricia Bay, near-shore (Site C) (Fig. 1, Supplementary Table 1). All samples were stored in plastic bags in a refrigerator at 4 °C. Sea-surface salinities and sea-surface temperatures were measured (Supplementary Table 1).

About 0.5–1 cm^3 of wet sediment was immersed in filtered seawater and after 1 min of sonication using an As One™ US-2R sonic bath the sediment was rinsed through a 20 μm Sanpo™ stainless steel sieve using filtered seawater. From this residue, the cyst fraction was separated using a density method (sodiumpolytungstate (SPT) at a density of 1.3 g cm^{-1} (Bolch, 1997)). Subsequently, single cysts were transferred using a micropippette to Nunclon 0.5 mL microwells, and incubated with an irradiance of 80 mmol photons m^{-2} s^{-1}, and a light:dark cycle of 16:8 h, filled with TL25 medium (Larsen et al., 1994) at temperatures and salinities comparable to the respective environments (Supplementary Table 1). Cysts were regularly checked for germination and observations of the cells were performed under an Olympus IX70 inverted light microscope (Olympus, Tokyo, Japan). Encysted and excysted cysts and vegetative stages were photographed and measured using an Olympus BX51 light microscope with a Nikon digital sight DS-1L 1 module, a Nikon Eclipse 80i microscope and coupled Nikon DS Camera Head (DS-Fi1)/DS Camera Control Unit

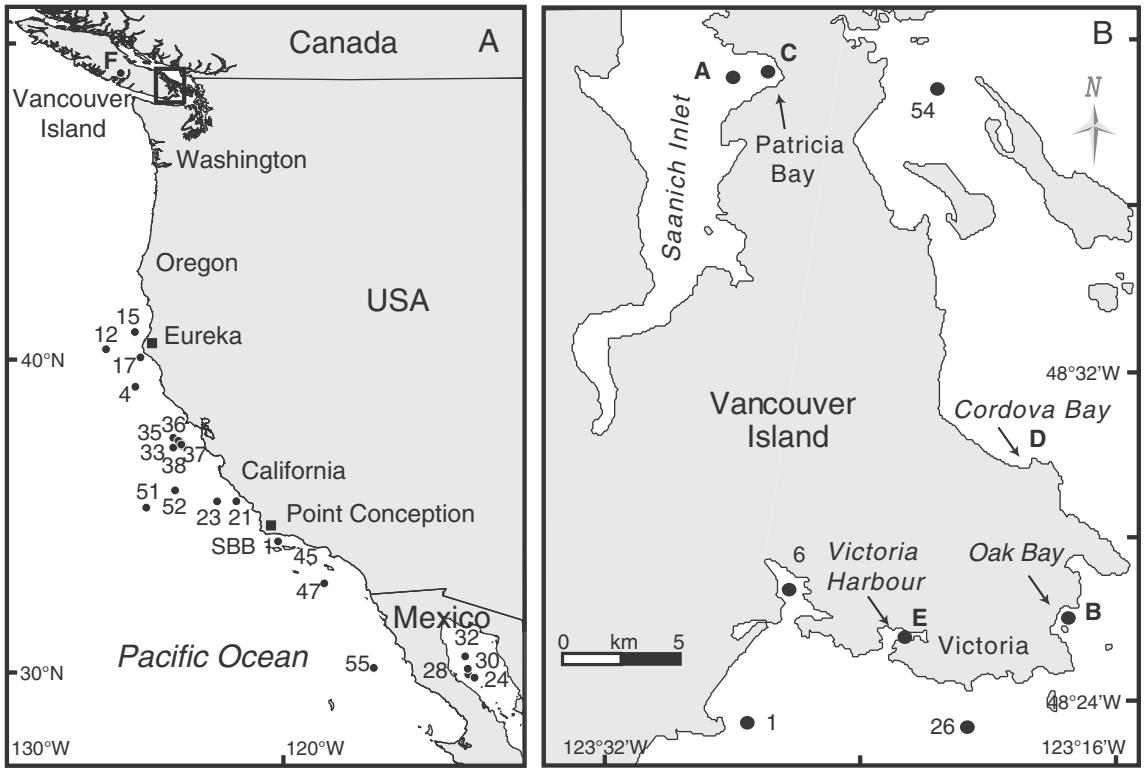

Fig. 1. A. Location of surface sediment sample sites along the NE Pacific margin containing cysts of *A. saanichi* (sites are numbered according to Pospelova et al., 2008), and the location of the Effingham Inlet sediment trap (site F). B. Map showing sampling locations for incubation experiments (site A to D), morphological measurements from the sediment trap in Saanich Inlet (also site A), and locations of surface sediments studied (sites are numbered according to Krepakevich and Pospelova, 2010). The location of Victoria Harbor used for sampling by Yamaguchi et al. (2011) is also shown (E).

DS-L2, and a Leica DM 5000 B equipped with a Leica DFC490 camera and Leica Application Suite 2.8.1 software, all with 100× oil immersion objectives. For every cyst, the average of the longest and shortest body diameter was measured and the average of four long processes, when possible. Also the number of processes per 10×10 μm was counted by centering a 10×10 μm grid on the surface of the cyst and counting all the processes within this grid.

2.2. Study of cysts from sediment trap samples and surface sediment

For further morphological measurements, sediment trap samples from the VENUS sediment trap in Saanich Inlet and the inner basin trap in Effingham Inlet were investigated (Fig. 1, Supplementary Table 1). Palynological techniques were used for processing (Pospelova et al., 2004; Price and Pospelova, 2011). The samples were oven-dried at 40 °C and then treated with room temperature 10% hydrochloric acid (HCl) to remove calcium carbonate particles. Material was rinsed twice with distilled water and sieved through 125 μm and retained on 15 μm nylon mesh to eliminate coarse and fine material. To dissolve siliceous particles, samples were treated with 48–50% hydrofluoric acid (HF) at room temperature for 2 days, and then treated for 10 min with HCl (10%) to remove fluorosilicates. The residue was rinsed twice with distilled water, sonicated for 30 sec and finally collected on a 15-μm mesh. Aliquots of residue were mounted in glycerine jelly.

All measurements and light microphotographs were obtained by K.N.M., V.P. and A.Y., respectively using an Olympus BX51 with a Nikon digital sight DS-1L 1 module, a Nikon eclipse 80i microscope and coupled Nikon DS Camera Head (DS-Fi1)/DS Camera Control Unit DS-L2 and a Leica DM 5000 B equipped with a Leica DFC490 camera and Leica Application Suite 2.8.1 software, all with 100× oil immersion objectives.

To determine the distribution of the studied spiny brown cysts, permanent slides of previously studied surface samples were reinvestigated, which included locations from coastal BC and from the NE Pacific (Supplementary Table 2).

2.3. Single-cell polymerase chain reaction (PCR) amplification and sequencing

For molecular investigations, two independent investigations were partaken. Four cells were isolated after germination of cysts isolated from Patricia Bay (Site C, Fig. 1) by A.Y. and one cell and one cyst were isolated from plankton from Cordova Bay (Site D, Fig. 1) by H.K using a slightly different method. These methods are detailed below. New sequences have been deposited in DDBJ/EMBL/GenBank under the accession numbers AB702985–AB702991.

2.3.1. LSU and SSU rDNA sequences of germinated cells by A.Y.

After germination of the cyst, one motile cell was isolated by micropipette under an inverted microscope, transferred to a glass slide with a vinyl tape frame (Horiguchi et al., 2000), and sealed with a cover glass. Cells were examined with a Zeiss Axioplan 2 microscope equipped with differential interference contrast (DIC) and connected to a Leica DC 500 color digital camera. After photographic records had been made, each cell was rinsed by transferring it through a series of drops of filtered seawater and finally a drop of distilled water. The cell was transferred to a 200 μL PCR tube containing 10 μL of Quick Extract™ FFPE DNA Extraction Solution (Epicentre, Madison, WI, USA) and incubated for 1 h at 56 °C, then for 2 min at 98 °C. The resulting extract was used as a DNA template for PCR amplification. The initial PCR was performed using a total volume of 25 μL and a PuRe Taq Ready-To-Go PCR bead (GE Healthcare Bio-Sciences, Québec, Canada). The parts of the SSU and LSU rRNA gene were amplified using universal eukaryote primers NPF1, 25F1 and LSU R2 (Kogame et al., 1999, Takano and Horiguchi, 2004, Chantangsi and Leander, 2010). The PCR protocol had an initial denaturation stage at 94 °C for 1 min; 35 cycles of denaturation at 94 °C for 30 s, annealing at 47 °C for 45 s, and extension at 72 °C for 45 s; and final extension at 72 °C for 7 min. The first PCR products were used as a DNA template for a nested or semi-nested PCR, where the following combinations of primer pairs were used separately: SR1b and SR5TAK, SR4 and SR9p, 25F1 and 25R1, LSU D3A and LSU R2 (Nunn et al., 1996; Yamaguchi and Horiguchi, 2005; Takano and Horiguchi, 2006; Yamaguchi et al., 2006). Thermal cycling was conducted using an initial denaturation stage at 94 °C for 1 min, followed by 30 cycles of 94 °C for 30 s, annealing at 47 °C or 55 °C for 30 s, and extension at 72 °C for 45 s, and final extension at 72 °C for 7 min. Amplified DNA fragments corresponding to the expected size were separated by agarose gel electrophoresis and cleaned using the UltraClean™ 15 DNA Purification Kit (Mo Bio Laboratories, CA, USA). The cleaned DNA was sequenced directly using the BigDye Terminator v3.1 cycle sequencing kit and Applied Biosystems 3730S 48-capillary sequencer. The results were confirmed by sequencing both forward and reverse strands.

2.3.2. SSU rDNA sequences of one cyst and one cell by H.K

After observation, the motile and cyst were isolated and placed in a 200-μL tube containing 5 μL distilled water. The cells were dried up after heating to 95 °C for 5 min within the tube. The dried cells were broken using a clean glass stick. PCR amplification was carried out in a 20-μL reaction volume with the reagents according to the manufacturer's recommendation for KOD-Plus-DNA Polymerase (Toyobo, Osaka, Japan) on a GeneAmp® PCR System 9700 (Applied Biosystems Japan, Tokyo, Japan). The PCR reactions were performed in two steps. The primer pair used in the first round of PCR to amplify the SSU rDNA region were SSU primer SR1 and LSU primer, 28-1483R (Nakayama et al., 1996, Daugbjerg et al., 2000). The product of the first round of PCR was used as a template for the second round, where the following combinations of primer pairs were used SSU and LSU primers, SR1 and SR5KAW, SR4 and SR9, and SR8KAW and SR12 (Nakayama et al., 1996; Kawami et al., 2006). The PCR product was purified using a Microcon YM-100 Centrifugal Filter Device (Millipore, Billerica, MA, USA), and the cycle-sequencing reaction was performed using an ABI PRISM BigDye™ Terminator v3.1 Cycle Sequencing Kit (Applied Biosystems, Foster City, CA, USA) following the manufacturer's protocol and sequenced with an ABI PRISM 310 Genetic Analyser.

2.3.3. Sequence alignments and phylogenetic analyses

SSU and LSU rDNA sequences were aligned using MacClade 4 (Maddison and Maddison, 2000) and visual fine tuning based on the datasets of Yamaguchi et al. (2011). The final alignment of SSU rDNA dataset consisted of 61 taxa and contained 1487 base pairs (*Archaeperidinium saanichi*). *Perkinsus marinus* was used as the outgroup species. The final alignment of the LSU rDNA dataset consisted of 48 taxa and contained 798 base pairs (*A. saanichi*), which region included the domains D1–D6, excluding the hypervariable part of domain D2. The apicomplexan *Neospora caninum* was used as outgroup. The GenBank accession numbers for all species used in the analyses are listed in Supplementary Table 3. The alignments are available from the authors upon request.

Phylogenetic trees for SSU and LSU rDNA were constructed using maximum likelihood (ML) and Bayesian analysis, respectively. For ML, the alignments were analyzed by GARLI version 0.951 (Zwickl, 2006). The Akaike information criterion as implemented in jModelTest 0.1.1. (Posada, 2008) indicated that the General Time Reversible (GTR) model of nucleotide substitution, with a gamma distributed rate of variation across sites and proportion of invariable sites was the most appropriate evolutionary model for the SSU datasets. The parameters were as follows: assumed nucleotide frequencies are $A=0.2597$, $C=0.1940$, $G=0.2422$, $T=0.3042$; substitution rate matrix with A–C substitutions $=1.3778$, A–$G=4.1789$, A–$T=1.2039$, C–$G=0.7401$, C–$T=7.6547$, G–$T=1.0000$; proportion of sites assumed to be invariable $=0.1960$ and rates for variable sites assumed to follow a gamma

distribution with shape parameter = 0.5730. For the LSU rDNA dataset, the GTR model of nucleotide substitution with a gamma distributed rate of variation across sites was chosen. The parameters were as follows: assumed nucleotide frequencies are $A = 0.2589$, $C = 0.1884$, $G = 0.2821$, $T = 0.2707$; substitution rate matrix with A–C substitutions = 1.3322, A–$G = 3.3025$, A–$T = 1.0905$, C–$G = 0.6440$, C–$T = 6.8377$, G–$T = 1.0000$; rates for variable sites assumed to follow a gamma distribution with shape parameter = 0.4850. Bootstrap analyses for both datasets were carried out for ML with 100 replicates to evaluate statistical reliability. MrBayes version 3.1.2 was used to perform Bayesian analyses on both SSU and LSU rDNA datasets (Huelsenbeck and Ronquist, 2001). The evolutionary model used in Bayesian analyses for SSU rDNA dataset was the GTR model with gamma-distributed rate variation across sites and a proportion of invariable sites, and the GTR model with a gamma distribution for LSU rDNA dataset. The program was set to operate four Monte-Carlo-Markov chains (MCMC) starting from a random tree. A total of 17,500,000 generations (SSU) and 1,500,000 generations (LSU) were calculated with trees sampled every 100 generations. The first 43,750 (SSU) and 3750 (LSU) trees in each run were discarded as burn-in. Posterior probabilities (PP) correspond to the frequency at which a given node was found in the post-burn-in trees.

3. Results

3.1. Germination experiments from coastal B.C. samples

Spiny brown cysts from samples from coastal B.C. were isolated and two species were identified: one large and one small. The cysts were incubated in *in situ* temperature and salinity conditions. Motile stage and cyst of the large species corresponded to a new species, *Archaeperidinium saanichi*, described below. The motile cells from cysts of the small species were similar with the motile cells identified as *Archaeperidinium minutum* by Yamaguchi et al. (2011), which were collected in Victoria Harbor, BC, Canada (Site E, Fig. 1). Because Yamaguchi et al. (2011) did not show the corresponding cyst, we describe the cyst below. Germinations were generally very fast, and took place after 1 or 2 days of incubation. Cells died relatively quickly a few days after germination and never divided.

3.2. Species description

SYSTEMATIC PALEONTOLOGY
Division DINOFLAGELLATA (Bütschli 1885)
Fensome et al., 1993
Class DINOPHYCEAE Pascher 1914
Subclass PERIDINIPHYCIDAE Fensome et al., 1993
Order PERIDINIALES Haeckel 1894
Family PROTOPERIDINIACEAE Fensome et al., 1993
Genus *Archaeperidinium* Jörgensen 1912 emend. A. Yamaguchi, Hoppenrath, Pospelova, T. Horiguchi & B.S. Leander 2011

Archaeperidinium saanichi Mertens, Yamaguchi, Kawami et Matsuoka (Plate 1, Figs. A–L) sp. nov.

Diagnosis: Motile cell: Length: 40.7 (45.3) 55.1 μm ($n = 9$), Width: 38.6 (43.0) 49.0 μm ($n = 9$). Tabulation formula: Po, X?, 4′, 2a, 7′′, 3c + t, 6 s, 5′′′, 2′′′′. The motile cell is slightly ovoidal with an apical horn but no antapical extension. Plates 1a and 2a are hexa, 2a and 4′′ are enlarged. S.d. plate does not touch the cingulum. Plates are microreticulate with scattered trichocyst pores.

Cyst (incubation): maximum central body diameter: 37.1 (45.0) 52.0 μm ($n = 20$), minimum central body diameter: 36.0 (43.0) 49.4 μm ($n = 20$), length of processes: 2.8 (5.4) 7.8 μm ($n = 72$). The cyst is spherical to subspherical, smooth and brown in color. If present, cell content typically has an orange hue. Numerous equidistant capitate, tapering, hollow processes which are never branched and have circular broad bases. Archeopyle theropylic and corresponds to the large 2a paraplate.

Holotype: Plate 1, Figs. A–L.

Type locality: Patricia Bay, Saanich Inlet, British Columbia, Canada (48° 25.508′, 123° 18.052′, 9 m water depth)

Etymology: The epithet reflects the name of the type locality of the species, Saanich Inlet.

3.3. Description

3.3.1. Morphology of motile cell

The motile cells are slightly ovoidal with an apical horn and no antapical extension (Plate 1, Fig. A), with the ventral side of hypotheca slightly less flattened (Plate 1, Fig. B). The cell content is pink in color and some cells have small orange pigment bodies underneath the thecal plates. The nucleus is located in the dorsal side of the epitheca. The microreticulate thecal plates carry trichocyst pores on the surface. Some of these pores are arranged parallel to the cingulum (Plate 1, Fig. C).

The plate arrangement of epitheca is asymmetrical. The circular apical pore plate (Po) is surrounded by a low collar formed by the raised edges of the second, third and fourth apical plates (2′, 3′ and 4′) (Plate 1, Fig. C). We could not confirm thecal boundaries of the canal plate (X) in this study. The first apical plate (1′) is rhombic (ortho-type) and asymmetrical (Plate 1, Fig. D). The anterior sides of plate 1′ are shorter than the posterior sides. Plate 2′ is pentagonal (Plate 1, Fig. E; 4′ also but not shown) and plate 3′ is irregular quadrangle (Plate 1, Fig. C). The two anterior intercalary plates are hexagonal and unequal in size (Plate 1, Figs. F–G). The first anterior intercalary plate (1a) is six-sided and located at the left side of the epitheca in dorsal view (Plate 1, Fig. G). The second anterior intercalary plate (2a) is twice the size of the 1a plate, and transversely elongated in the dorsal side of the epitheca (Plate 1, Fig. F).

The precingular series consists of seven plates. The first, third and seventh precingular plate (1′′, 3′′ and 7′′) are four-sided (Plate 1, Figs. D, G). The cingular side of plate 1′′ is shorter than that of plate 7′′. The second and the fourth precingular plates (2′′ and 4′′) are five-sided (Plate 1, Figs. E–F). Plate 4′′ is wide and its contact with plate 2a is longer than its contact with plate 1a (F Plate 1, Fig. F).

The cingulum is slightly right-handed (ascending), lined with narrow lists (Plate 1, Fig. H). The long and narrow transitional plate (t) is positioned between the first cingular plate (C1) and the anterior sulcal plate (S.a.) (Plate 1, Fig. H). Plate C1 is of similar width as plate 1′′. The second cingular plate (C2) is the widest of the cingular plate series. The third cingular plate (C3) is of similar width as the fifth postcingular plate (5′′′) (Plate 1, Fig. I).

The sulcus is flat and consists of four large plates. The S.a. is long and narrow and its anterior part intruded between plates 1′′ and 7′′ (Plate 1, Fig. H). The right-sulcal plate (S.d.) does not reach the cingulum (Plate 1, Fig. H). The distinct accessory plate (fin) expands from the left side of the S.d. plate (Plate 1, Fig. J). This fin covers the sulcal area and extended posteriorly beyond the cell (Plate 1, Fig. J). The left sulcal plate (S.s.) is long and forms a J-shaped curve (Plate 1, Fig. H). The anterior part of S.s. connects with the S.a. and the transitional plate (t) (Plate 1, Fig. H). The posterior sulcal plate (S.p.) is asymmetrical V-shaped (Plate 1, Fig. H, I).

The plate arrangement of the hypotheca is also asymmetrical. The cells have five postcingular plates. The fifth postcingular plate (5′′′) is wider than the first postcingular plate (1′′′). The third postcingular plate (3′′′) is five-sided and positioned below the 4′′ plate (Plate 1, Fig. K). Plate 3′′′ and 4′′ have similar widths (Plate 1, Fig. K). The antapical series is composed of two plates (Plate 1, Fig. L).

The plate formula is thus Po, X?, 4′, 2a, 7′′, 3c + t, 6 s, 5′′′, 2′′′′, and the complete tabulation is illustrated in Figs. 2–4 (except for the plate X).

3.3.2. Dimensions

The motile cells measure 40.7 (45.3) 55.1 μm in length (including apical horn, stdev = 5.0, $n = 9$) and 38.6 (43.0) 49.0 μm in width (stdev = 3.6, $n = 9$).

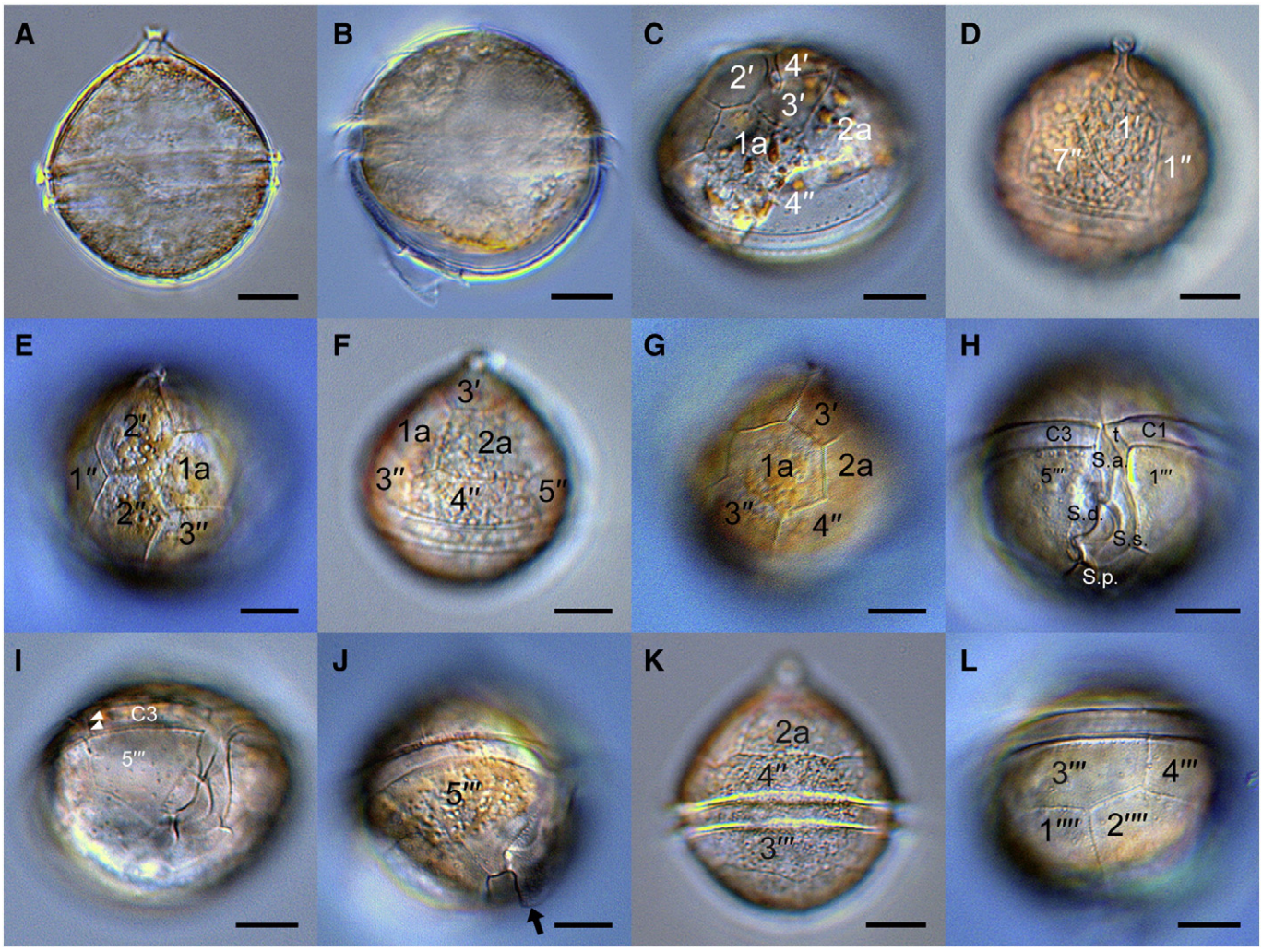

Plate 1. Figs. A–L: Motile stage of *Archaeperidinium saanichi* after germination of cysts from Patricia Bay, Saanich Inlet (Holotype). A. Mid-ventral view showing general shape. B. Lateral view showing nucleus and fin. C. Dorsal view showing pores and arrangement of two anterior intercalary plates and apical plates 2′–4′. D. Ventral view showing rhombic, asymmetric 1′ and four-sided 1″ and 7″. E. Dorsal view showing pentagonal 2′. F–G. Dorsal views showing anterior intercalary plates and some of the precingular plates. H. Ventral view showing ascending cingulum and sulcal plates: anterior sulcal plate (S.a.), right-sulcal plate (S.d.), left sulcal plate (S.s.), posterior sulcal plate (S.p.), transitional plate (t). I. View of third cingular plate (C3) Double arrowheads indicate the boundary line of C2 and C3. J. View of hypotheca, indicating position of fin (arrow). K. View of position of 3‴ *vs.* 4″. L. View of hypotheca showing both antapical plates 1⁗ and 2⁗. All scale bars are 10 μm.

3.3.3. Synonyms

Balech (1964a, as *Peridinium minutum* Kofoid, 1907, Plate 1, Figs. 1–10).

Okolodkov (2005, as *Protoperidinium minutum* (Kofoid, 1907) Loeblich 1970, p. 289, Figs. 12, 28).

3.3.4. Morphology of cyst of *A. saanichi*

3.3.4.1. Description. The resting cysts are spherical to subspherical and dark brown when cell content is present and hazelbrown when empty (compare Plate 2, Fig. A and B). The living cysts have abundant orange granules (Plate 2, Fig. A). The wall is thin. The cyst surface is smooth and densely packed with numerous equidistant, non-tabular processes (15 (19.5) 22 processes per 10×10 μm, stdev = 2.7, $n = 8$). Sometimes bumps or reduced processes can be observed between processes (Plate 2, Fig. H). Processes are capitate, always ending with distal expansions and tapering, hollow and generally erect, although these can be slightly recurved. The processes are never fused or never branched at the end. The process bases are circular in cross-section (Plate 2, Fig. A, Fig. H). The archeopyle is intercalary and theropylic and corresponds to the large 2a paraplate (Plate 2, Figs. C–D, F).

3.3.4.2. Dimensions. Measurements of 20 cysts that germinated and gave rise to *A. saanichi* cells show that the maximum diameter of the central body varies between 37.1 (45.0) and 52.0 μm (stdev = 3.8 μm, $n = 20$), minimum diameter between 36.0 (43.0) and 49.4 μm (stdev = 4.1 μm, $n = 20$), and the length of processes between 2.8 (5.4) and 7.8 μm (stdev = 1.0 μm, $n = 72$) (Fig. 5). Similar measurements were obtained from cysts from sediment trap samples from Saanich Inlet and Effingham Inlet: the maximum diameter of the central body varies between 41.8 (49.0) 57.6 μm (stdev = 3.9 μm, $n = 50$), minimum diameter between 41.5 (47.3) and 57.6 μm (stdev = 3.5 μm, $n = 50$) and the length of processes between 2.5 (4.9) and 7.6 μm (stdev = 1.0 μm, $n = 200$) (Fig. 5).

3.4. Morphology of cyst of *A. minutum* sensu Yamaguchi et al. (2011)

3.4.1. Description

The cysts that were incubated from coastal B.C., are spherical to subspherical and dark brown when cell contents are still present and light brown when empty (compare Plate 3, Fig. A and Plate 3, Figs. B–F). Empty cysts also appear darker when they were covered in mucus (Plate 3, Figs. G–I). The living cysts have abundant reddish

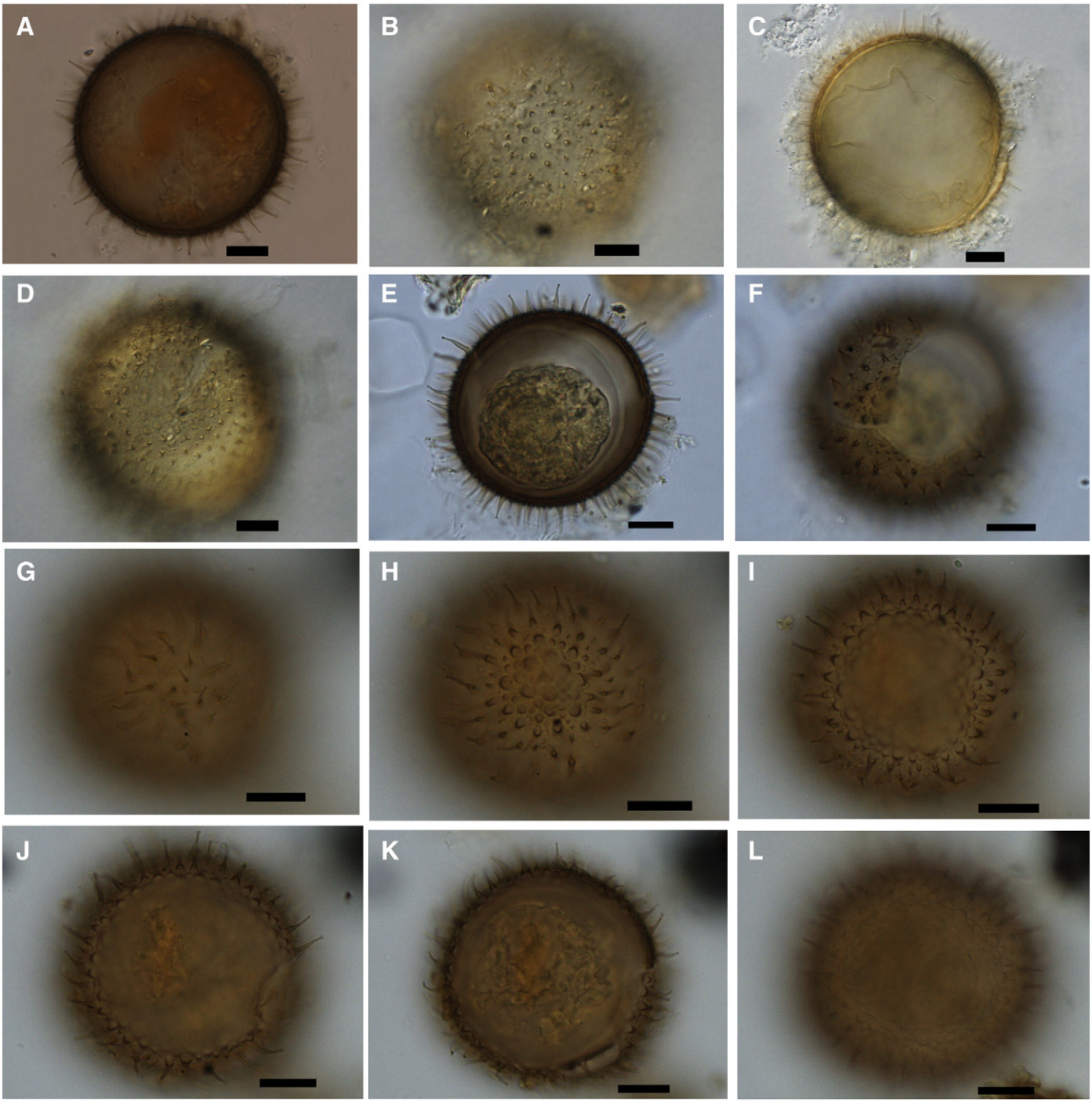

Plate 2. Figs. A–L: Cysts of *Archaeperidinium saanichi* from coastal BC. A. Live cyst with orange granules from Oak Bay (Site B). B–D. Germinated cyst from culture showing processes and 2a archeopyle on lower focus (C–D). E–F. Cyst from surface sediment sample from Esquimalt Harbor (UVic 08-005) showing cross section with tipped processes and endospore present (E) and missing operculum, showing a 2a archeopyle. G–L. Cyst from surface sediment sample from Cowichan Bay, Saanich Inlet (UVic 07-924, Site S13), progressive upper to lower focus showing distinct tipped processes with wide bases. Arrows in G point to processes surrounded by bumps arranged in polygons. All scale bars are 10 μm.

granules (Plate 3, Fig. A). The wall is thin. The cyst surface is smooth and densely packed with numerous equidistant, non-tabular, processes (20 (24.3) 30 processes per 10×10 μm, stdev = 4.0, $n = 10$). Under light microscope, the processes appear distally solid with pericoels extending variable distance along process length, however as Ribeiro et al. (2010) showed by SEM observations, it is possible that processes are hollow. Sometimes bumps can be observed between processes (Plate 3, Fig. G, I), which can be arranged in a polygonal pattern around the spines (Plate 3, Fig. G) and is similar to polygonal patterns observed on the theca of *P. minutum* (Dodge 1983, his Fig. 8). Processes are acuminate or capitate with distal expansions, tapering and erect. The processes are never fused or branched at the end. The process bases are circular in cross-section (Plate 3, Fig. G, I). The archeopyle, which is the only expression of tabulation on the cyst, is intercalary and theropylic and corresponds to the 2a paraplate (Plate 3, Fig. C).

3.4.2. Dimensions

Measurements of cysts of *A. minutum* sensu Yamaguchi et al. (2011) from coastal B.C. that germinated show that the maximum diameter of the central body varies between 24.3 (30.2) and 33.1 μm (stdev = 2.4 μm, $n = 15$), minimum central body diameter between 24.0 (29.2) and 32.2 μm (stdev = 2.4 μm, $n = 15$), and the length of processes

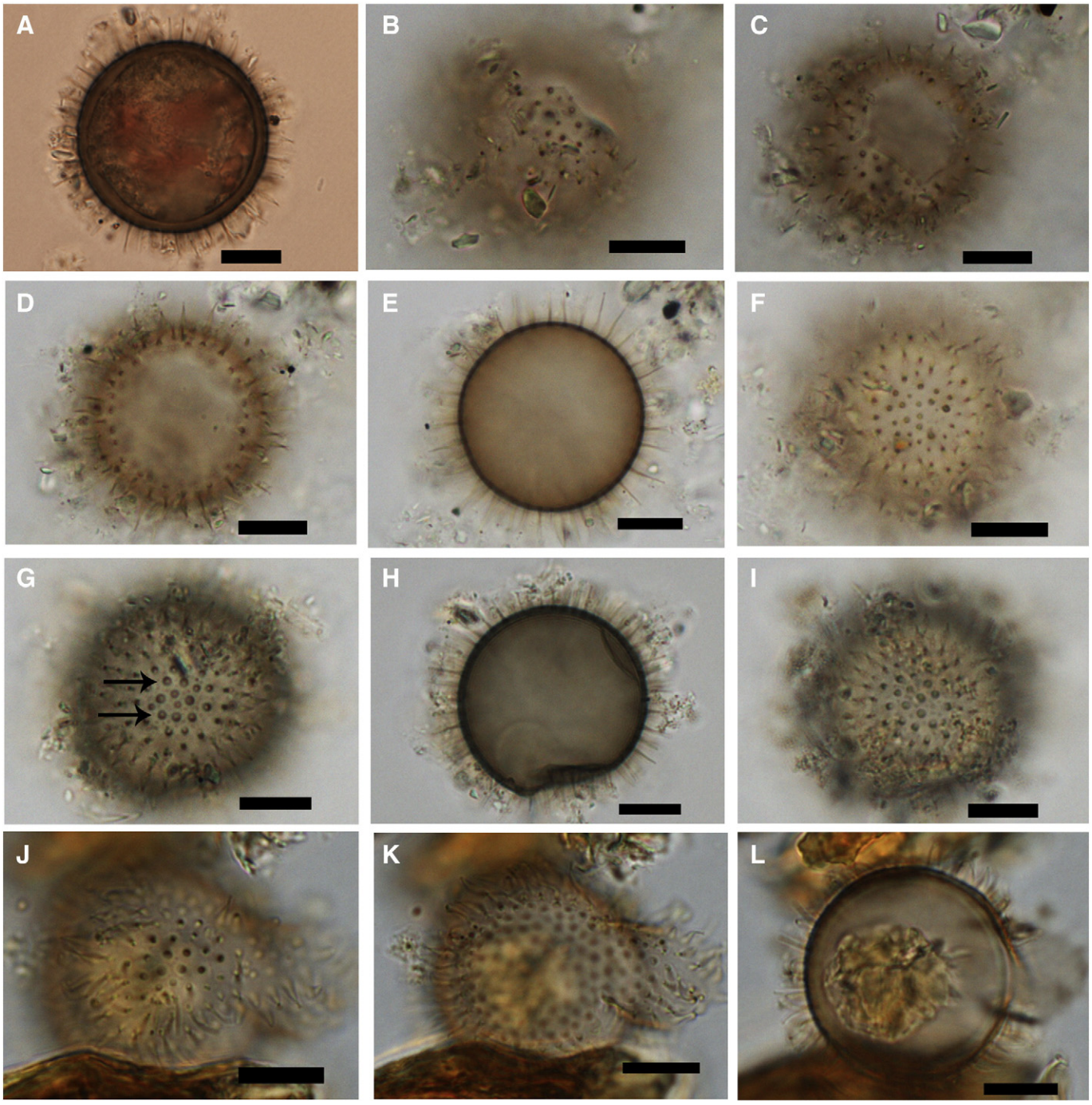

Plate 3. Figs. A–L: Cyst of *Archaeperidinium minutum sensu* Yamaguchi et al. 2011 from coastal BC. A. Live cyst with red granules from Patricia Bay, Saanich Inlet (Site C). B–F. Germinated cyst from Patricia Bay, Saanich Inlet (Site C), progressive upper to lower focus showing 2a archeopyle. G–I. Germinated cyst from Patricia Bay, Saanich Inlet (Site C), progressive upper to lower focus, with short bumps around processes as indicated by arrows. J–L. Cyst from Cowichan Bay, Saanich Inlet (UVic 07-911) showing 2a archeopyle. All scale bars are 10 μm.

between 3.4 (5.1) and 7.2 μm (stdev = 0.9 μm, $n = 60$) (Fig. 5). Similar measurements were obtained from cysts from sediment trap samples from Saanich Inlet and Effingham Inlet: the maximum diameter of the central body varies between 24.5 (29.7) and 33.9 μm (stdev = 2.1 μm, $n = 50$), the minimum central body diameter between 24.4 (29.3) and 33.8 μm (stdev = 2.1 μm, $n = 50$) and the length of processes between 2.0 (4.9) and 7.7 μm (stdev = 1.0 μm, $n = 200$) (Fig. 5).

3.5. Molecular data and phylogeny

SSU rDNA. We obtained 1239 bp (A.Y. from theca), 1785 bp (H.K., from cyst) and 1762 bp (H.K., from theca) from three cells (Accession number: AB702985, AB702986, AB702987) and they did not have any differences. We used the longest sequence (Accession number: AB702986) for the phylogenetic analyses (Fig. 6). The SSU rDNA sequence of *A. saanichi* has slight substitutions among the sequences of *A. minutum* by Ribeiro et al. (2010) GQ227501 and Yamaguchi et al. (2011) AB564308 and AB564309 (2–4 base pairs out of 1556 base pairs). Both ML and Bayesian analyses show that *A. saanichi* and three sequences of *A. minutum* form a clade. This clade is a sister group to *Amphidiniopsis dragescoi* and *Herdmania litoralis* is positioned at the base of this clade. The species within the family Protoperidiniaceae fall into four well-supported clades (Fig. 6). These clades were concordant with Clades I-IV named by Ribeiro et

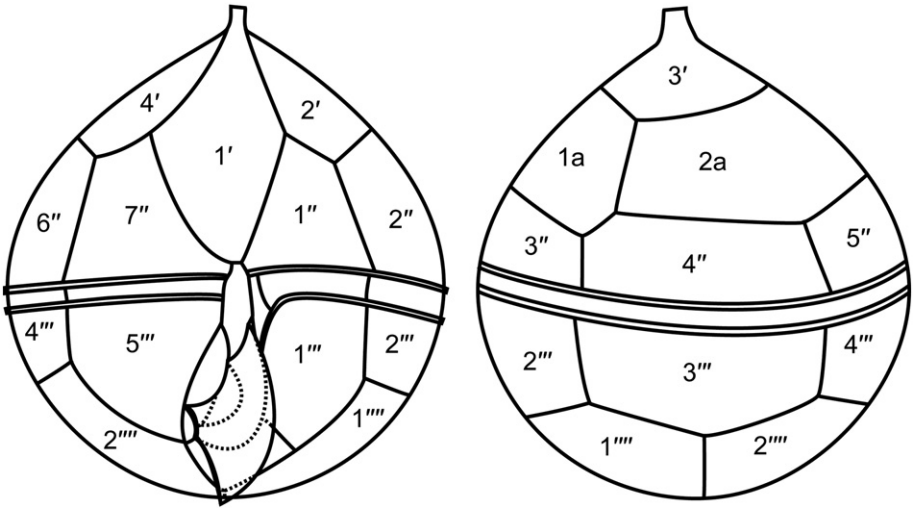

Fig. 2. Drawing of interpreted tabulation showing ventral (left) and dorsal (right) sides. Labels: 1′ to 4′, apical plates; 1″ to 7″, precingular plates; 1a and 2a, anterior intercalary plates; 1‴ to 5‴, postcingular plates; 1⁗ and 2⁗, antapical plates.

al. (2010) and Yamaguchi et al. (2011). The clade comprised of *A. saanichi*, *A. minutum*, *A. dragescoi* and *H. litoralis* is referred to as Clade IV (Fig. 6). The deep branches in the tree were short and without statistical support from either ML bootstrapping (<50%) or Bayesian PP (<0.95).

LSU rDNA. We obtained 1197, 1128, 1243 and 1195 base pairs from four germinated motile cells (Accession numbers: AB702988, AB702989, AB702990, AB702991) and they are identical. We used the longest sequence for the phylogenetic analyses (Fig. 7). The LSU rDNA sequence of *A. saanichi* has six substitutions out of 1233 base pairs with *A. minutum* by Ribeiro et al. (2010) (Accession number GQ227502). The LSU rDNA sequence of *A. minutum* by Yamaguchi et al. (2011) contains three deletion sites comparing to the sequences of *A. saanichi* and *A. minutum* by Ribeiro et al. (2010). Except for these deletion and unambiguous sites, there are three substitutions out of 980 base pairs between *A. saanichi* and *A. minutum* by Yamaguchi et al. (2011). As result of ML and Bayesian analyses, *A. saanichi* and two sequences of *A. minutum* form a clade, and *H. litoralis* is positioned at the base of this clade (Clade D, 97% ML bootstrap and 1.00 Bayesian PP). The clade formed by the same sections as clade I in the SSU rDNA analysis was well-supported (Clade A). Clade B comprised the section *Oceanica* plus *P. steidingerae* was moderately supported (61% ML bootstrap and 1.00 Bayesian PP).

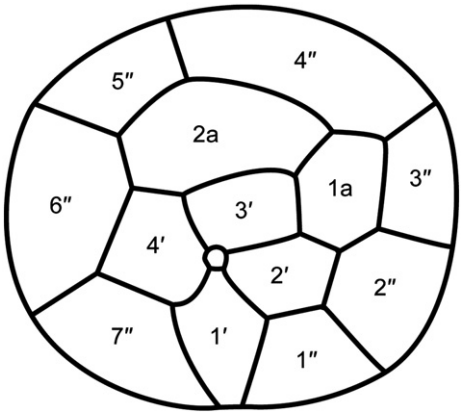

Fig. 3. Drawing of interpreted tabulation of epitheca. Labels: 1′ to 4′, apical plates; 1″ to 7″, precingular plates; 1a and 2a, anterior intercalary plates. Since we could not confirm thecal boundaries of the canal plate (X) in this study, so it is not shown in the drawing.

Two diplopsalid species (*Diplopsalis lenticula* and *Preperidinium meunieri*), which previously formed a clade in Yamaguchi et al. (2011) and referred to as Clade C, do not cluster together in this study, as well as the in result of Ribeiro et al. (2010).

3.6. Distribution of cysts of *A. saanichi*

Cysts of *A. saanichi* have a wide geographical distribution in the NE Pacific (Supplementary Table 2, Fig. 1). This species is a common component of the dinoflagellate cyst assemblages in estuarine waters of southern British Columbia (Canada) and coastal waters on the NE Pacific, with an average relative abundance of ~1%. Cysts of *A. saanichi* have been found in surface sediment samples corresponding to sea surface temperatures between 5 °C and 17 °C and sea surface salinities between 22 and 35 psu. The highest abundance of cysts of *A. saanichi* has been recorded in surface sediments of Patricia Bay in Saanich Inlet (see Cyst type L in Price and Pospelova, 2011), where

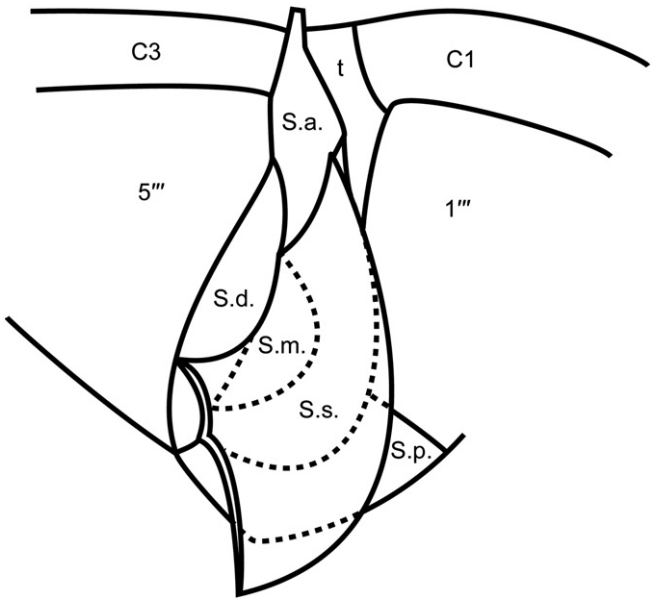

Fig. 4. Drawing of interpreted sulcal tabulation. Labels: C1 and C3, cingular plates; 1‴ and 5‴, postcingular plates; S.a., anterior sulcal plate; S.d., right sulcal plate; S.p., posterior sulcal plate; S.m., median sulcal plate., S.s., left sulcal plate; t, transitional plate.

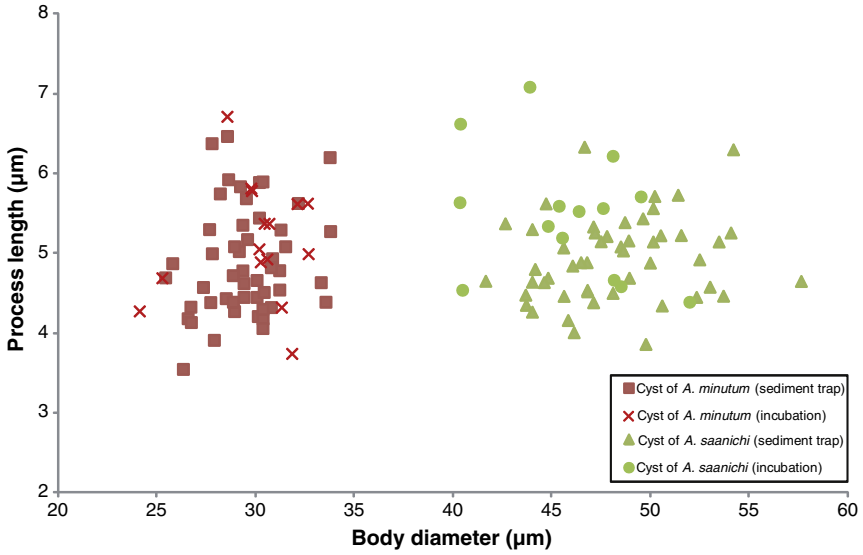

Fig. 5. Measurements of body size and process length for cysts isolated for incubation experiments and from sediment traps of cyst of *Archaeperidinium saanichi* (resp. filled circles and triangles) and cysts of *Archaeperidinium minutum* sensu Yamaguchi et al. 2011 (resp. crosses and squares) showing two distinct clusters.

it contributes from 5% to 20% of the cyst assemblages with an average concentration of 4100 cysts g^{-1} (V.P., A.P. unpublished data), and where optimal conditions corresponded to winter sea surface temperatures between 5 °C and 10 °C and winter sea surface salinities between 23 psu and 28 psu.

4. Discussion

4.1. Comparison of motile stage of A. saanichi to other species

It is clear that the shape of the intercalary plates is a consistent feature used in the definitions of related species: species have been either described as having more or less symmetrical[2] or asymmetrical intercalary plates. This characteristic can be used as a first step to compare this species to others. This feature is however not consistent for descriptions of *A. minutum* in the available literature, although the original description shows symmetrical intercalary plates (Kofoid, 1907). We think this characteristic should be used to distinguish *A. saanichi* (pronounced asymmetrical intercalaries) from other species in the *A. minutum* complex (symmetrical to slightly asymmetrical intercalaries). *Archaeperidinium saanichi* then corresponds to *A. minutum* depicted by Balech (1964a, as *Peridinium minutum* Kofoid, 1907, Plate 1, Figs. 1–10) and by Okolodkov (2005, as *Protoperidinium minutum* (Kofoid, 1907) Loeblich, 1970, p. 289, Fig. 12, 28). These are re-designated as *Archaeperidinium saanichi* and are slightly ovoidal, have the same pronounced asymmetry in the two intercalary plates and a S.d. that does not reach the cingulum.

Archaeperidinium saanichi differs from *A. minutum sensu* Fukuyo et al. (1977, as *Protoperidinium minutum* (Kofoid, 1907) Loeblich, 1970, p. 14, Figs. 3–10), *sensu* Ribeiro et al. (2010, as *Protoperidinium minutum* (Kofoid, 1907) Loeblich, 1970, p. 53, Figs. 22–23) and *sensu* Yamaguchi et al. (2011, as *Archaeperidinium minutum*, p. 107–109, Figs. 12–23, 30) by being more rounded, having only slight asymmetry in the subequal intercalary plates and having an S.d. that reaches the cingulum. The motile cells germinated from the small species of cysts from Saanich Inlet were all similar to specimens described by Yamaguchi et al. (2011), and we confirmed that they had subequal intercalary plates and a S.d. that reaches the cingulum. They are similar to the original description of *A. minutum* in Kofoid (1907, p. 310, Plate 31, Figs. 42–45). Although it is difficult to confirm whether the S.d. reaches the cingulum in the holotype of *A. minutum* by Kofoid (1907, p. 310, Plate 31, Figs. 42–45), we consider these to be examples of *A. minutum*. Other descriptions and/or depictions cannot be assigned to either species and need reinvestigation. For instance, specimens depicted by Nie (1939, Fig. 12, p. 592) could be representative of both *A. saanichi* and *A. minutum* as one depicted S.d. does, and another does not reach the cingulum and there is a pronounced asymmetry shown in the epitheca. Balech (1964a, p. 25, not illustrated) and Taylor (1976, p. 137, Plate 33, Fig. 372) mention the occurrence of both types of asymmetry, but do not show the position of the S.d.. Several other publications that show and/or discuss this species do not address these characteristics: Kisselew (1950, p. 158, Fig. 239), Margalef et al. (1955, p. 95, Figs. i–j), Silva, (1957, p. 29, Plate 4, Figs. 7–8), Halim (1967, p. 741, Plate 9, Figs. 125–126), Wall and Dale (1968, p. 278, Plate 3, Fig. 32, Plate 4, Figs. 6–7), Wood (1968, p. 104, Fig. 311) and Hernández-Becerril (1991).

Other species with symmetrical intercalary plates can easily be differentiated on this basis from *A. saanichi*. *Peridinium monospinum* Paulsen, 1907 (p. 12, Fig. 11, copied in Paulsen, 1908, p. 41–42, Fig. 41) has been depicted in the original description as having two symmetrical subequal intercalary plates and all subsequent descriptions: Lebour (1925, p. 107, Plate XVI, Figs. 3a–3h) (copied by Peters 1930, p. 71, Fig. 38), Dangeard (1927, p. 347, Fig. 13a,b), Wailes (1928, p. 4, Figs. 42, 43), Silva (1949), (p. 344, Plate 5, Figs. 12–13) and Zonneveld and Dale (1994, p. 361, Fig. 1). Zonneveld and Dale (1994) reinstated this species because they observed a specific type of cyst and a typical reticulation on the theca, not observed on *A. minutum*. A significant problem with this species, remarked by Balech (1964b), is that in the original drawing by Paulsen (1907) the 1a is connected to 1′′, which is not the case in any of the other depicted *P. monospinum*. This together with the fact that *P. monospinum* has been considered a synonym of *A. minutum* by a number of authors, makes all these subsequent descriptions questionable. *P. monospinum* clearly needs further investigation. Because of the distinctness of the species of Zonneveld and Dale (1994), we call this "*P. monospinum*" *sensu* Zonneveld and Dale (1994). This species is quite similar to

[2] Such symmetry of the intercalaries is also shown by Schiller (1935), p. 141, which copies from previous publications (slightly asymmetrical specimens depicted in Zonneveld and Dale (1994) are badly copied from Schiller (1935)).

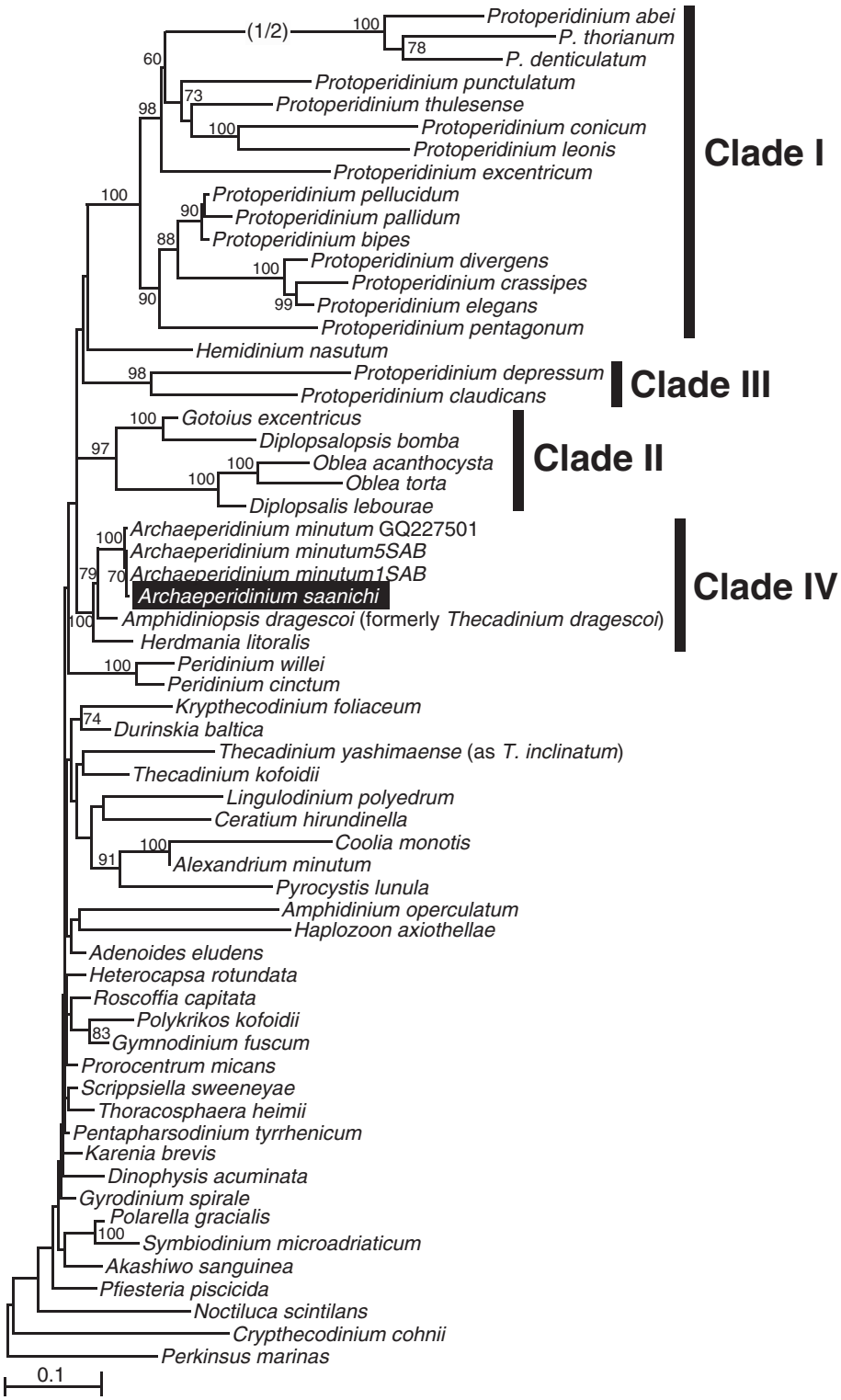

Fig. 6. Maximum-likelihood (ML) tree of dinoflagellates inferred from SSU rDNA sequences. ML bootstrap values over 50% are shown. Thick branches indicate Bayesian posterior probabilities (PP) over 0.95. Clades I–IV are labeled and marked with vertical lines on the right. The scale bar represents inferred evolutionary distance in changes/site. The DNA sequence generated in this study is indicated in the black box. The branch leading to fast-evolving species have been halved (indicated by 1/2).

Properidinium aspinum Meunier, 1919 (p. 55, Plate 18, Figs. 33–36), which was considered a synonym of *P. monospinum* by Lebour (1925). However, this species cannot be *P. monospinum* because 1a does not touch 1″. Therefore we consider this another valid species, which is characterized by distinct reticulations, a S.d. that reaches the cingulum, symmetrical intercalaries and epi- and hypotheca of unequal size (which makes it different from "*P. monospinum*" *sensu* Zonneveld and Dale, 1994). *Protoperidinium constrictum* (Abé, 1936) Balech 1974, as described by Abé, 1936 (as *Peridinium constricta*, p. 676–680, Figs. 75–83) also has symmetrical intercalaries and was considered a synonym of *P. monospinum* by Abé (1981, p. 307); however we consider it different from the holotype because it does not

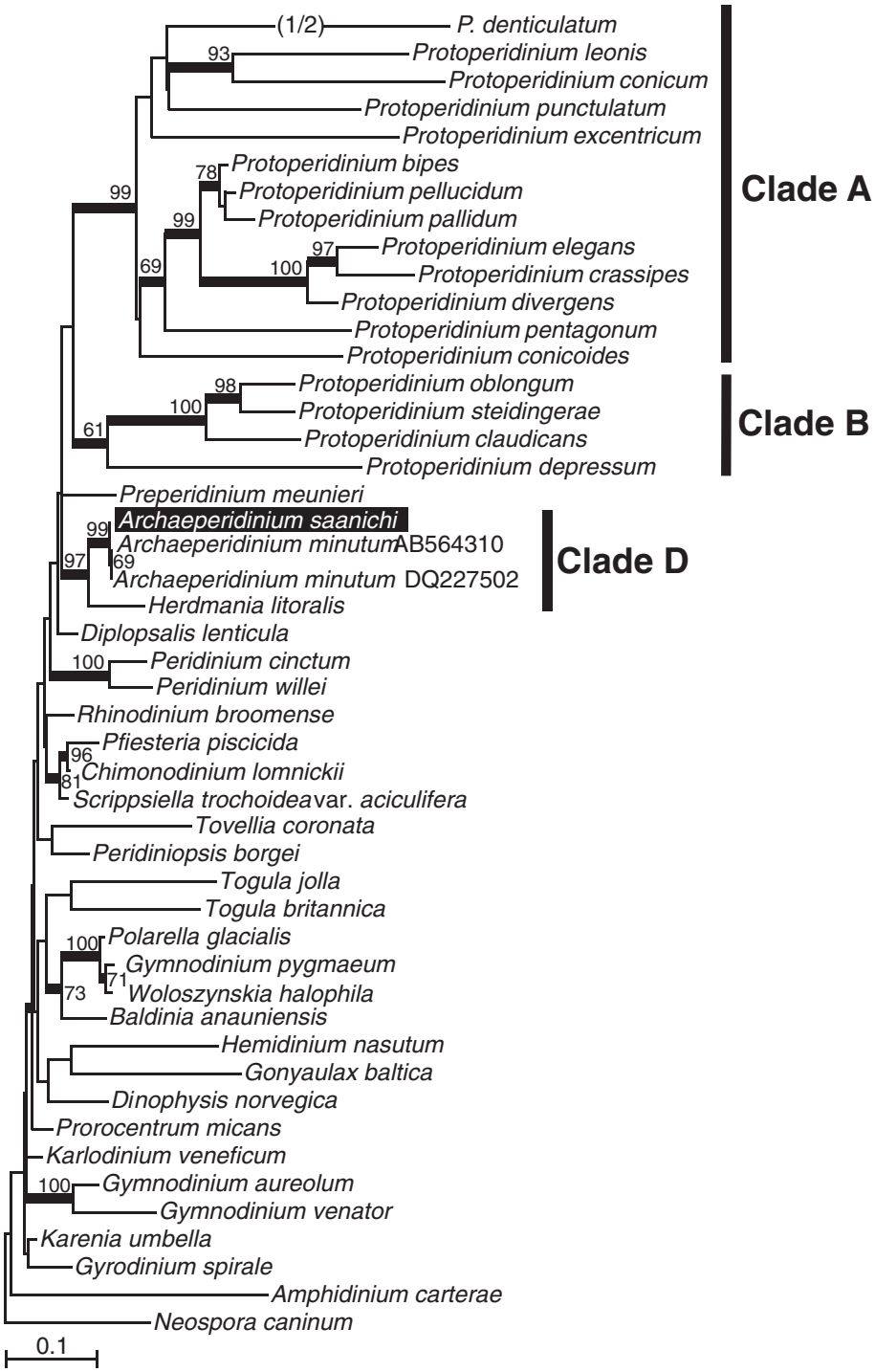

Fig. 7. Maximum-likelihood tree inferred from LSU rDNA sequences. ML bootstrap values (ML) over 50 and Bayesian posterior probabilities (PP) over 0.95 are shown at the nodes (ML/PP). Clades A, B and D are labeled and marked with vertical lines on the right. The scale bar represents inferred evolutionary distance in changes/site. The DNA sequence generated in this study is indicated in the black box. The branch leading to fast-evolving species have been halved (indicated by 1/2).

have a 1a connected to 1″ and from the specimen reinstated by Zonneveld and Dale (1994) because it has a different size and a S.d. not reaching the cingulum. *Protoperidinium talihouense* (Fauré-Fremiet 1908) Balech 1994 as described by Fauré-Fremiet (1908, as *P. minutum* var. *talihouensis*, p. 227, Fig. 13) is also symmetrical but has an extra small precingular plate (8″) and different shape of 1′ than *A. minutum* (Balech 1994).

It also differs from other species that have been described with pronounced asymmetrical intercalary plates. It is different from *Protoperidinium aspidiotum* Balech, 1964b as described by Balech (1964b, Plate 1I, Figs. 15–23, copied in Balech, 1988, p. 82, Plate 21, Figs. 1–3) which is smaller (35–39 μm × 34–35 μm), has a larger and more pointed fin and a S.d. plate that reaches the cingulum. It is also different from *Protoperidinium mendiolae* Balech, 1978 which is larger (53–71 μm × 53–72 μm in diameter), less rounded and pentagonal in shape and has a S.d. that reaches the cingulum (Balech, 1978, p. 5, Figs. 1–15). It also differs from *Protoperidinium mutsuense* (Abé 1936) Balech 1974 because that species has one large 1a.

Protoperidinium asymmetricum (Abé 1927) Balech 1974 also has such an enlarged 1a, but also has a prominent diagonal suture ridge in the epitheca (Abé 1927, as *Spherodinium asymmetria*, p. 391, Figs. 11–13). A key can be used to differentiate the species (Fig. 8).

4.2. Comparative morphology of cysts

The cyst of *A. saanichi* can be easily distinguished from the cyst belonging to the motile stage of *A. minutum sensu* Yamaguchi et al., 2011 (small cyst) using morphological measurements of cyst body size, with a cut-off value of 37 μm (Fig. 5). Processes of both cyst types are of similar length (Fig. 5), being hollow, tapering and capitate, probably always ending in aculeate ends, same as observed by Ribeiro et al. (2010, p. 54, Figs. 4–5, p. 55, Fig. 13). Processes of cysts of *A. saanichi* are somewhat more expanded though than cysts of *A. minutum* sensu Yamaguchi et al. (2011), clearly having wider bases (compare Plate 2, Figs. A–L and Plate 3, Figs. A–L), and on average a slightly lower number of processes. Furthermore, both cysts have a 2a type archeopyle type, although it is evident that the size of the archeopyle varies between these species, where the archeopyle is much larger in cysts of *A. saanichi*.

The cysts of *A. minutum sensu* Yamaguchi et al. (2011) have previously been described as cysts of *Protoperidinium minutum* by Price and Pospelova (2011, p.11, Plate 5, their Figs. 1–2). Cysts described by Ribeiro et al. (2010, as cysts of *Protoperidinium minutum*) are of nearly equal dimensions with a diameter of 25 (30) 34 μm ($n=27$) and process lengths of 4 (6) 9 μm ($n=17$). Fukuyo et al. (1977) described a similar small cyst (28–32 μm) with curved acuminate spines (3–5 μm) and a theropylic intercalary archeopyle. These cysts are very similar to cysts described here of *A. minutum sensu* Yamaguchi et al. (2011), aside from the fact that no distal expansions are shown on the drawing by Fukuyo et al. (1977), as earlier remarked by Ribeiro *et al.* (2010). These are, however, easily overlooked using light microscopy, but SEM images always show the presence of these expansions (Ribeiro et al., 2010). Therefore, SEM investigations of these cysts are needed to investigate the possibility of ultrastructural characteristics to differentiate these types.

The cyst of *A. saanichi* has previously been depicted as *Echinidinium* spp. by Krepakevich and Pospelova (2010, Plate 2, Fig. e) and as "cyst type L" by Price and Pospelova (2011, p. 10, Plate 4, their Figs. 7–9).

Other spiny brown cysts described in the literature can be easily distinguished from cysts of *A. saanichi* and *A. minutum* since the archeopyle type (2a) of both cysts is unique among spiny brown cysts. However, because the archeopyle is often not visible, and the fact that many of the described archeopyle types of the other described species need verification, other characters such as the body diameter, number of spines and distribution, and spine length or structure (e.g. striations) should be used. The cysts of *A. minutum* are quite similar to *Echinidinium delicatum* Zonneveld, 1997 but according to Zonneveld (1997) *E. delicatum* has a different archeopyle and is smaller (17–25 μm) than the cyst shown by Fukuyo et al. (1977). The cyst of *Protoperidinium tricingulatum* Kawami et al., 2009 is similar in size and process lengths to *A. minutum* but only has 15 processes per 10×10 μm^2 (compared to 30 for *A. minutum*). The processes are mostly solid except at the base and the archeopyle is a slit. The cyst of *A. monospinum* sensu Zonneveld and Dale, 1994 is spherical (28–40 μm) and covered with many randomly distributed processes of two different types (one larger, hollow, capitate with bifurcated ends; the other solid, acuminate). The cyst opens with a slit-like archeopyle (theropylic). It is similar in size to *A. minutum* but differs in the archeopyle type, number and type of processes.

4.3. Phylogenetic position of Archaeperidinium saanichi as inferred from rDNA sequences

Ribosomal DNA sequences from dinoflagellates are relatively conserved, which limits the utility of these particular markers for delimiting closely related species from one another and for inferring close relationships within the group (e.g. Saldarriaga et al. 2004; Shalchian-Tabrizi et al. 2006). The nuclear encoded SSU and LSU rDNA sequences showed only slight differences between *Archaeperidinium minutum* and *A. saanichi*, Other examples of two morphologically distinct dinoflagellate species with identical or similar rDNA sequences have been documented by Logares et al. (2007) for the brackish dinoflagellate *Scrippsiella hangoei* and the freshwater species *Peridinium*

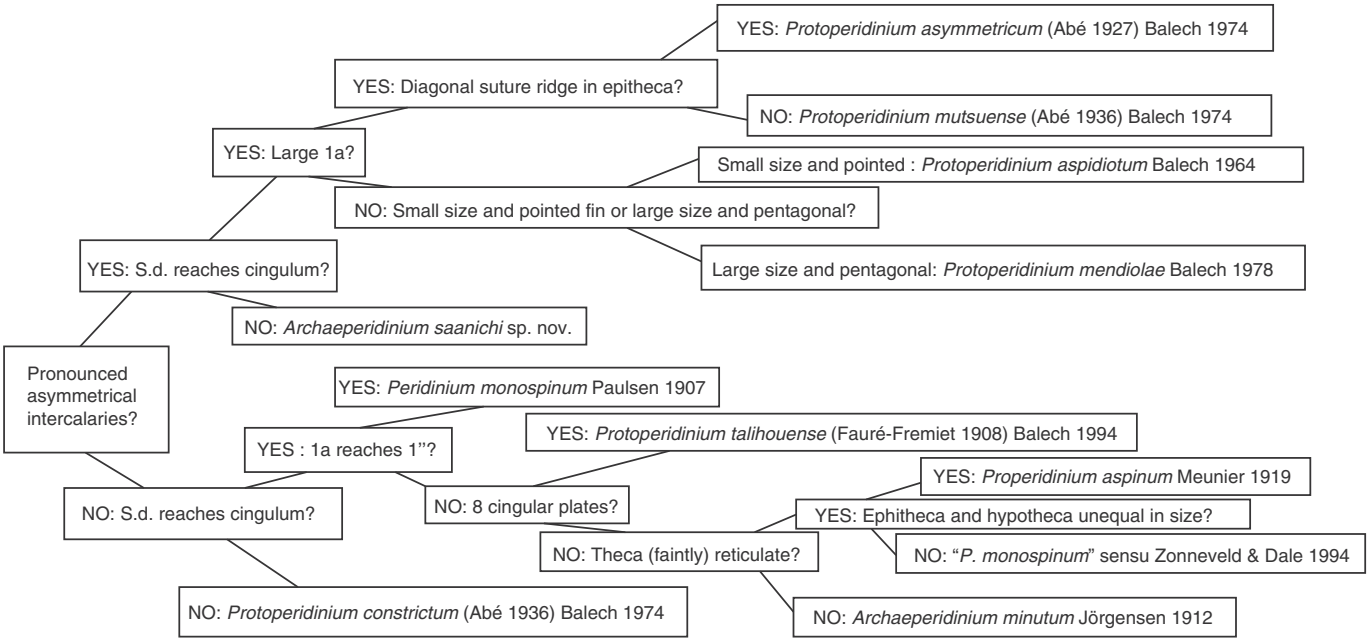

Fig. 8. A flowchart of a key to differentiate all closely related species.

aciculiferum and by Moestrup et al. (2008) for freshwater species *Borghiella dodgei* and *Borghiella tenuissima*. Logares et al. (2007) showed that the internal transcribed spacer regions (ITS1, ITS2), SSU, and partial LSU rDNA sequences between *S. hangoei* and *P. aciculiferum* were identical, despite their pronounced morphological differences. However, genetic separation of the two species was indicated from an almost 2% sequence divergence of the mitochondrial cytochrome *b* gene, in addition to differences in the amplified fragment length polymorphism (AFLP) pattern. Moestrup et al. (2008) showed that the LSU rDNA sequences of *B. dodgei* and *B. tenuissima* had only slight genotypic diversity, although they are morphologically very different. Logares et al. (2007) concluded that identical rDNA sequences in *S. hangoei* and *P. aciculiferum* could be the result of rapid divergence where time has been too short for any neutral fixations in the populations. In light of this hypothesis by Logares et al. (2007), Moestrup et al. (2008) suggested that enough time has passed since *B. dodgei* and *B. tenuissima* diverged to allow for some neutral fixations, thus revealing minor LSU rDNA sequence divergences. We consider that between *A. saanichi* and *A. minutum* there has likely been also not enough evolutionary time since diverge to fix changes at the rDNA level, in a way similar to that of *B. dodgei* and *B. tenuissima*.

4.4. Distribution of *A. saanichi*

The cyst stage is here only described by cyst-theca experiments from coastal British Columbia (Canada). We have found similar cysts over a long stretch of the NE Pacific (Fig. 1), and a relatively broad range of temperature (5–17 °C) and salinity (22–35 psu). A recent sediment trap study from Saanich Inlet (Price and Pospelova 2011) shows that the cyst of *A. saanichi* occurs throughout the year with slightly higher cyst fluxes in the winter months at temperatures between 5 and 10 °C and salinities between 23–28 psu, while the cyst of *A. minutum sensu* Yamaguchi et al. (2011) has the greatest flux during summer months (July–August) at a temperature between 15 and 19 °C and salinity around 29 psu. This suggests that *A. saanichi* has a preference for cooler temperatures and lowered salinities, and *vice versa* for *A. minutum sensu* Yamaguchi et al. (2011).

It is likely that the species abundance, like most heterotrophic dinoflagellates, is also determined by its prey availability, likely diatoms, ciliates, dinoflagellates and other protists (e.g. Jacobson and Anderson, 1986, 1992, 1996; Bockstahler and Coats, 1993; Hansen and Calado, 1999), which could be indirectly regulated by macronutrient availability. A similar relation has been proposed for the large heterotrophic cyst species *Selenopemphix undulata* (Verleye et al., 2011).

5. Conclusions

Archaeperidinium saanichi sp. nov. is described here from coastal British Columbia (Canada) through incubation experiments of a larger spiny brown cyst. The motile stage is characterized by pronounced asymmetrical intercalary plates, S.d. not touching the cingulum and its large size. We show that the theca of *A. saanichi* is different from other closely related species in the asymmetry of the intercalary plates and the size and the position of S.d. plate. We also show that the cyst morphology of this species is similar to both the cyst belonging to the motile stage of *A. minutum* as described by Ribeiro et al. (2010) and by Yamaguchi et al. (2011) (which we describe here), having a 2a archeopyle and aculeate process tips, but can be distinguished in the size of archeopyle and body diameter, as well as the shape and number of processes. The LSU and SSU rDNA sequences show the close affiliation of *A. saanichi* to *A. minutum*, but are too conserved to distinguish the two species from one another. Accordingly, we provide a key to differentiate all species within the *A. minutum* complex. *A. saanichi* is suggested to have a preference for cooler temperatures and lowered salinities.

Acknowledgements

Kenneth Neil Mertens is a postdoctoral fellow of FWO Belgium and this research was partly conducted at Nagasaki University and was supported by a Kakenhi grant 22-00805. Aika Yamaguchi was supported by a postdoctoral research salary from the Assembling the Tree of Life grant (NSF #EF-0629624) and operating funds to B.S.L. from the National Science and Engineering Research Council of Canada (NSERC 283091-09) and the Canadian Institute for Advanced Research, Programs in Evolutionary Biology and Integrated Microbial Biodiversity. This research was partly supported by NSERC's Discovery (224236) and Ship Time grants to Vera Pospelova. Andre Catrijsse (VLIZ, Belgium) is thanked for providing us with surface sediment samples from the North Sea which unfortunately did not contain any spiny brown cysts. One Effingham Inlet sediment trap sample was kindly provided by Dr. R. Timothy Patterson (Carleton University, Canada). The VENUS (Victoria Experimental Network Under the Sea) team is thanked for their assistance with collection of Saanich Inlet sediment trap material, and surface sediments from Site A in Patricia Bay. Surface sediment samples from the NE Pacific were provided by the Scripps Institution of Oceanography (SIO), Oregon State University (OSU), Monterey Bay Aquarium Research Institute (MBARI) and U.S. Geological Survey (USGSMP). The authors like to thank the editor, André Rochon and one anonymous reviewer for suggestions that significantly improved the paper.

Appendix A. Supplementary data

Supplementary data associated with this article can be found in the online version, at http://dx.doi.org/10.1016/j.marmicro.2012.08.002. These data include Google maps of the most important areas described in this article.

References

Abé, T.H., 1927. Report of the biological survey of Mutsu Bay. 3. Notes on the protozoan fauna of Mutsu Bay. I. Peridiniales. Science Reports of the Tohoku Imperial University, Fourth Series, Biology, Sendai, Japan 2 (4), 383–438.

Abé, T.H., 1936. Report of the Biological Survey of Mutsu Bay. 29. Notes on the Protozoan Fauna of Mutsu Bay. II. Genus *Peridinium*; subgenus *Archaeperidinium*. Science Reports of the Tohoku Imperial University, Fourth Series, Biology 10 (4), 639–686.

Abé, T.H., 1981. Studies on the family Peridiniidae. An unfinished monograph of armoured Dinoflagellata: Publications of the Seto Marine Biological Laboratory, Special Publication Series, vol. VI, pp. 1–413.

Balech, E., 1964a. Tercera contribucion al conocimiento del genero "*Peridinium*". Revista del Museo Argentino de Ciencias Naturales "Bernardino rivadavia" e Instituto Nacional de Investigacion de las Ciencias Naturales, Hidrobiología 1 (6), 179–201 (In Spanish).

Balech, E., 1964b. El plancton de Mar del Plata durante el periodo 1961–1962 (Buenos Aires, Argentina). Instituto de Biologia Marina Boletin 4, 1–49 (In Spanish).

Balech, E., 1974. El genero "Protoperidinium" Bergh, 1881 ("Peridinium" Ehrenberg, 1831, Partim). Revista del Museo Argentino de ciencias naturales "Bernardino Rivadavia" e Instituto nacional de las ciencias naturales. Hirdobiología 4 (1), 1–79.

Balech, E., 1978. *Protoperidinium (Archaeperidinium) mendiolae* n. sp. Neotropica 24 (71), 3–7 [In Spanish].

Balech, E., 1988. Los dinoflagellados del Atlantico sudoccidental. Publicaciones Especiales Instituto Español de Oceanografia 1, 1–310 (In Spanish).

Balech, E., 1994. Contribucion a la taxonomia y nomenclatura del genero Protoperidinium (Dinoflagellata). Revista del Museo Argentino de Ciencias naturales "Bernardino Rivadavia", Hidrobiologia 7 (4), 61–80 (In Spanish).

Bockstahler, K.R., Coats, D.W., 1993. Spatial and temporal aspects of mixotrophy in Chesapeake Bay dinoflagellates. Journal of Eukaryotic Microbiology 40, 49–60.

Bolch, C.J.S., 1997. The use of polytungstate for the separation and concentration of living dinoflagellate cysts from marine sediments. Phycologia 37, 472–478.

Bolch, C.J.S., 2001. PCR protocols for genetic identification of dinoflagellates directly from single cysts and plankton cells. Phycologia 40 (2), 162–167.

Chantangsi, C., Leander, B.S., 2010. An SSU rDNA barcoding approach to the diversity of marine interstitial cercozoans, including descriptions of four novel genera and nine novel species. International Journal of Systematic and Evolutionary Microbiology 60, 1962–1977.

Dangeard, P., 1927. Phytoplancton de la Croisière du SYLVANA (Février-Juin 1913). Annales de l'Institut Océanographique de Monaco 4 (8), 287–407.

Daugbjerg, N., Hansen, G., Larsen, J., Moestrup, Ø., 2000. Phylogeny of some of the major genera of dinoflagellates based on ultrastructure and partial LSU rDNA sequence data, including the erection of three new genera of unarmoured dinoflagellates. Phycologia 39, 302–317.

Dodge, J.D., 1983. Ornamentation of thecal plates in *Protoperidinium* (Dinophyceae) as seen by scanning electron microscopy. Journal of plankton research 5 (2), 119–127.
Fauré-Fremiet, E., 1908. Étude descreptive des Péridiniens et des Infusoires Ciliés du Plancton de la Baie de la Hougue. Annales des Sciences Naturelles (Zool.) Série 9 (7) 209–242 + Pl. 15–16. [In French].
Gómez, F., 2005. A list of free-living dinoflagellate species in the world's oceans. Acta Botanica Croatica 64 (1), 129–212.
Fukuyo, Y., Kittaka, J., Hirano, R., 1977. Studies on the cysts of marine dinoflagellates — I *Protoperidinium minutum* (Kofoid) Loeblich. Bulletin of the Plankton Society of Japan 24, 11–18.
Halim, Y., 1967. Dinoflagellates of the South-East Carribean Sea (East Venezuela). Internationale Revue für die gesamte Hydrobiologie 52 (5), 701–755.
Hansen, P.J., Calado, A.J., 1999. Phagotrophic mechanisms and prey selection in free living dinoflagellates. Journal of Eukaryotic Microbiology 46, 382–389.
Head, M.J., 1996. Modern dinoflagellate cysts and their biological affinities. In: Jansonius, J., McGregor, D.C. (Eds.), Palynology: Principles and Applications. American Association of Stratigraphic Palynologists Foundation, pp. 1197–1248.
Head, M.J., Harland, R., Matthiessen, J., 2001. Cold marine indicators of the late Quaternary: the new dinoflagellate cyst genus *Islandinium* and related morphotypes. Journal of Quaternary Science 16, 621–636.
Hernández-Becerril, D.U., 1991. *Protoperidinium* (Dinophyceae) species in the Gulf of California and off the coasts of Baja California. Annales del Instituto de Ciencias del Mar y Limnología 18 (1), 77–88.
Hoppenrath, M., Yubuki, N., Bachvaroff, T.R., Leander, B.S., 2010. Re-classification of *Pheopolykrikos hartmannii* as *Polykrikos* (Dinophyceae) based partly on the ultrastructure of complex extrusomes. European Journal of Protistology 46, 29–37.
Horiguchi, T., Yoshizawa-Ebata, J., Nakayama, T., 2000. *Halostylodinium arenarium*, gen. et sp. nov. (Dinophyceae), a coccoid sand-dwelling dinoflagellate from subtropical Japan. Journal of Phycology 36, 960–971.
Huelsenbeck, J.P., Ronquist, F., 2001. MRBAYES: Bayesian inference of phylogenetic trees. Bioinformatics 17, 754–755.
Jacobson, D.M., Anderson, D.M., 1986. Thecate heterotrophic dinoflagellates: feeding behaviour and mechanisms. Journal of Phycology 22, 249–258.
Jacobson, D.M., Anderson, D.M., 1992. Ultrastructure of the feeding apparatus and myonemal system of the heterotrophic dinoflagellate *Protoperidinium spinulosum*. Journal of Phycology 28, 69–82.
Jacobson, D.M., Anderson, D.M., 1996. Widespread phagocytosis of ciliates and other protists by marine mixotrophic and heterotrophic thecate dinoflagellates. Journal of Phycology 32, 279–285.
Jörgensen, E., 1912. Bericht über die von der schwedischen hydrographisch-biologischen Kommission in den schwedischen Gewässern in den Jahren 1909–10 eingesammelten Planktonproben. Svenska Hydrografisk-Biologiska Kommissionens Skrifter 4, 1–20.
Kawami, H., Matsuoka, K., 2009. A new cyst-theca relationship of *Protoperidinium parthenopes* Zingone and Montresor (Peridiniales, Dinophyceae). Palynology 33 (2), 11–18.
Kawami, H., Iwataki, M., Matsuoka, K., 2006. A new diplopsalid species *Oblea acanthocysta* sp. nov. (Peridiniales, Dinophyceae). Plankton Benthos Research 1, 183–190.
Kawami, H., Van Wezel, R., Koeman, R.P., Matsuoka, K., 2009. *Protoperidinium tricingulatum* sp. nov. (Dinophyceae), a new motile form of a round, brown, and spiny dinoflagellate cyst. Phycological Research 57, 259–267.
Kisselew, I.A., 1950. Armored flagellates (Dinoflagellata) from marine and fresh waters of the USSR. Identification guide to the USSR fauna. published by Zoological Institute of the USSR (Russian) Academy of Sciences, Moscow and Leningrad . [In Russian].
Kofoid, C.H., 1907. Dinoflagellata of the San Diego Region, III. Descriptions of new species. Contributions from the Laboratory of the Marine Biological Association of the United Kingdom XVII. University of California Publications. Zoology 3, 299–340.
Kogame, K., Horiguchi, T., Masuda, M., 1999. Phylogeny of the order Scytosiphonales (Phaeophyceae) based on DNA sequences of rbcL, partial rbcS, and partial LSU rDNA. Phycologia 38, 496–502.
Krepakevich, A., Pospelova, V., 2010. Anthropogenic impact on coastal bays of Southern Vancouver Island (BC, Canada) as reflected in phytoplankton sedimentary records. Continental Shelf Research 30 (18), 1924–1940.
Larsen, N.H., Moestrup, Ø., Pedersen, P.M., 1994. Scandinavian Culture Centre for Algae and Protozoa. Catalogue 1994. Department of Phycology. Botanical Institute. University of Copenhagen.
Lebour, M.V., 1925. The Dinoflagellates of Northern Seas. Marine Biological Association, Plymouth, UK.
Loeblich III, A.R., 1970. The amphiesma or dinoflagellate cell covering. Proceedings of the North American Paleontological Convention, Chicago, 1969, Part G, pp. 867–929.
Logares, R., Rengefors, K., Kremp, A., Shalchian-Tabrizi, K., Boltovskoy, A., Tengs, T., Shurtleff, A., Klaveness, D., 2007. Phenotypically different microalgal morphospecies with identical ribosomal DNA: a case of rapid adaptive evolution? Microbial Ecology 53, 549–561.
Maddison, D.R., Maddison, W.P., 2000. MacClade 4: Analysis of Phylogeny and Character Evolution Version 4.0. Sinauer Associates, Sunderland, MA.
Margalef, R., Durán, M., Saiz, P., 1955. El fitoplancton de la ría de Vigo. Investigación Pesquera 2, 85–129 (In Spanish).
Matsuoka, K., 1988. Cyst-theca relationships in the diplopsalid group (Peridiniales, Dinophyceae). Review of Palaeobotany and Palynology 56, 95–122.
Matsuoka, K., Fukuyo, Y., 1986. Cyst and motile morphology of a colonial dinoflagellate *Pheopolykrikos hartmannii* (Zimmermann) comb. nov. Journal of Plankton Research 8 (4), 811–818.
Matsuoka, K., Noriko, N., Kawami, H., Iwataki, M., 2006b. New method for establishing the cyst-motile form relationship in dinoflagellates. Fossils 80, 33–40 [In Japanese].
Matsuoka, K., Kawami, H., Fujii, R., Iwataki, M., 2006a. Further examination of the cyst-theca relationship of *Protoperidinium thulesense* (Peridiniales, Dinophyceae) and the phylogenetic significance of round brown cysts. Phycologia 45, 632–641.
Meunier, A., 1919. Microplancton de la mer Flamande. 3. Les Péridiniens. Mémoires du Musée Royal d'Histoire Naturelle de Belgique 8 (1), 1–116 [In French].
Moestrup, Ø., Hansen, G., Daugbjerg, N., 2008. Studies on Woloszynskioid Dinoflagellates III: on the ultrastructure and phylogeny of *Borghiella dodgei* gen. et sp. nov., a cold-water species from Lake Tovel, N. Italy, and on *B. tenuissima* comb. nov. (syn. *Woloszynskia tenuissima*). Phycologia 47 (1), 54–78.
Nakayama, T., Watanabe, S., Mitsui, K., Uchida, H., Inouye, I., 1996. The phylogenetic relationship between the Chlamydomonadales and Chlorococcales inferred from 18S rDNA sequence data. Phycological Research 44, 47–55.
Nie, D., 1939. On the thecal morphology of *Peridinium*, with special reference to the ventral area. Science (Science Society of China) 23, 584–600 [In Chinese].
Nunn, G.B., Theisen, B.F., Christensen, B., Arctander, P., 1996. Simplicity-correlated size growth of the nuclear 28S ribosomal RNA D3 expansion segment in the crustacean order Isopoda. Journal of Molecular Evolution 42, 211–223.
Okolodkov, Y.B., 2005. *Protoperidinium* Bergh (Dinoflagellata) in the southeastern Mexican Pacific Ocean: part I. Botanica Marina 48, 284–296.
Paulsen, O., 1907. The Peridiniales of the Danish Waters. Meddelelser fra Kommissionen for Havundersøgelser Serie: Plankton 1 (5), 1–26.
Paulsen, O., 1908. XVIII. Peridiniales. In: Brandt, K., Apstein, C. (Eds.), Nordisches Plankton. Botanischer Teil, Lipsius und Tischler, Kiel und Leipzig, pp. 1–124.
Peters, N., 1930. Peridinea. Die Tierwelt der Nord- und Ostsee, 17(2.d2). Akademische Verlagsgesellschaft: Leipzig 13–84 pp.v [In German].
Posada, D., 2008. jModelTest: phylogenetic model averaging. Molecular Biology and Evolution 25, 1253–1256.
Pospelova, V., Chmura, G.L., Walker, H.A., 2004. Environmental factors influencing spatial distribution of dinoflagellate cyst assemblages in shallow lagoons of southern New England (USA). Review of Paleobotany and Palynology 128 (1–2), 7–34.
Pospelova, V., de Vernal, A., Pedersen, T.F., 2008. Distribution of dinoflagellate cysts in surface sediments from the northeastern Pacific Ocean (43–25°N) in relation to sea-surface temperature, productivity and coastal upwelling. Marine Micropaleontology 68 (1–2), 21–48.
Price, A.M., Pospelova, V., 2011. High-resolution sediment trap study of organic-walled dinoflagellate cyst production and biogenic silica flux in Saanich Inlet (BC, Canada). Marine Micropaleontology 80 (1), 18–43.
Ribeiro, S., Lundholm, N., Amorim, A., Ellegaard, M., 2010. *Protoperidinium minutum* (Dinophyceae) from Portugal: cyst–theca relationship and phylogenetic position on the basis of single-cell SSU and LSU rDNA sequencing. Phycologia 49 (1), 48–63.
Saldarriaga, J.F., Taylor, F.J.R., Cavalier-Smith, S., Menden-deuer, S., Keeling, P.J., 2004. Molecular data and the evolutionary history of dinoflagellates. European Journal of Protistology 40, 85–111.
Schiller, J., 1935. Dinoflagellatae (Peridineae) in monographischer Behandlung. Dr. L.Rabenhorst's Kryptogamen-Flora von Deutschland, Österreich und der Schweiz. Bd. 10(3): Teil, 2(1), pp. 1–160.
Shalchian-Tabrizi, K., Minge, M.A., Cavalier-Smith, T., Nedreklepp, J.M., Klaveness, D., Jakobsen, K.S., 2006. Combined heat shock protein 90 and ribosomal RNA sequence phylogeny supports multiple replacements of dinoflagellate plastids. Journal of Eukaryotic Microbiology 53, 217–224.
Silva, E. de S., 1949. Diatomáceas e dinoflagelados da Baia de Cascais. Portugaliae Acta Biologica (série B, Sistemática) 18, 300–382 (In Portugese).
Silva, E. de S., 1957. Dinoflagelados do plancton marinho de Angola. Sparata dos "Anais" Junta de Investigações Ultramar 10 (2), 3–80 (In Portugese).
von Stosch, H.A., 1973. Observations on vegetative reproduction and sexual life cycles of two freshwater dinoflagellates, *Gymnodinium pseudopalustre* Schiller and Woloszynskia apiculata sp. nov. British Phycological Journal 8, 105–134.
Takano, Y., Horiguchi, T., 2004. Surface ultrastructure and molecular phylogenetics of four unarmored heterotrophic dinoflagellates, including the type species of the genus *Gyrodinium*. Phycological Research 52, 107–116.
Takano, Y., Horiguchi, T., 2006. Acquiring scanning electron microscopical, light microscopical and multiple gene sequence data from a single dinoflagellate cell. Journal of Phycology 42, 251–256.
Taylor, F.J.R., 1976. Dinoflagellates from the International Indian Ocean Expedition. Bibliotheca Botanica 132. E. Schweizerbart'sche Verlagsbuchhandlung, Stuttgart.
Verleye, T.J., Pospelova, V., Mertens, K.N., Louwye, S., 2011. The geographical distribution and (palaeo)ecology of *Selenopemphix undulata* sp. nov., a new late Quaternary dinoflagellate cyst from the Pacific Ocean. Marine Micropaleontology 78, 65–83.
Wailes, G.H., 1928. Dinoflagellates from British Columbia with Descriptions of New Species. Study from the Stations of the Biological Board of Canada. Part I. With Plates 1–3. Vancouver Museum Notes 3 (1), 20–31.
Wall, D., Dale, B., 1968. Modern dinoflagellate cysts and evolution of the Peridiniales. Micropaleontology 14 (3), 265–304.
Wood, E.J.F., 1968. Dinoflagellates of the Caribbean Sea and Adjacent Areas. University of Miami Press, Coral Gables, Florida.
Yamaguchi, A., Horiguchi, T., 2005. Molecular phylogenetic study of the heterotrophic dinoflagellate genus *Protoperidinium* (Dinophyceae) inferred from small subunit rRNA gene sequences. Phycological Research 53, 30–42.
Yamaguchi, A., Kawamura, H., Horiguchi, T., 2006. A further phylogenetic study of the heterotrophic dinoflagellate genus *Protoperidinium* (Dinophyceae) based on small and large subunit ribosomal RNA gene sequences. Phycological Research 54, 317–329.

Yamaguchi, A., Hoppenrath, M., Pospelova, V., Horiguchi, T., Leander, B.S., 2011. Molecular phylogeny of the marine sand-dwelling dinoflagellate *Herdmania litoralis* and an emended description of the closely related planktonic genus *Archaeperidinium* Jörgensen. European Journal of Phycology 46 (2), 98–112.

Zonneveld, K.A.F., 1997. New species of organic-walled dinoflagellate cysts from modern sediments of the Arabian Sea (Indian Ocean). Review of Palaeobotany and Palynology 97, 319–337.

Zonneveld, K.A.F., Dale, B., 1994. The cyst–motile stage relationships of *Protoperidinium monospinum* (Paulsen) Zonneveld et Dale comb. nov. and *Gonyaulax verior* (Dinophyta, Dinophyceae) from the Oslo Fjord (Norway). Phycologia 33, 359–368.

Zwickl, D.J., 2006. Genetic algorithm approaches for the phylogenetic analysis of large biological sequence datasets under the maximum likelihood criterion. Ph.D. dissertation, The University of Texas at Austin.